PERGAMON

Carbon 39 (2001) 559–567

CARBON

Effects of pre-carbonization on porosity development of activated carbons from rice straw

Chang Hun Yun[a], Yun Heum Park[a], Chong Rae Park[b,*]

[a]*Department of Textile Engineering, Sung Kyun Kwan University, Suwon 440-764, South Korea*
[b]*Hyperstructured Organic Materials Research Center and Enviro-Polymers Design Laboratory, Department of Fiber and Polymer Science, Seoul National University, Seoul 151-742, South Korea*

Received 19 August 1999; accepted 17 June 2000

Abstract

To investigate the pre-carbonization effect on the porosity development in activated carbons, two types of activated carbons were manufactured from rice straws by the one-stage and two-stage processes, respectively. Despite of the differences in thermal history of the two processes, pore-drilling and pore-widening occurred simultaneously to increase the micro and mesopore volumes up to the activation temperature of 800°C, above which pore-widening effect was however dominant, leading to the increase of mesopore volume. The micropore volume of the one-stage activated carbons (denoted S1AC) was considerably decreased, whereas that of the two-stage activated carbons (denoted S2AC) rarely changed with the increase of activation time. S2AC exhibited higher values of the BET surface area, micro and mesopore volumes than those of S1AC. This was attributed to the effect of the pre-carbonization that ensures the formation of relatively less defective carbonaceous structures. © 2001 Published by Elsevier Science Ltd.

Keywords: A. Activated carbon; B. Carbonization

1. Introduction

Activated carbons can be manufactured from various raw materials such as wood [1], coal [2], some polymers [3,4], and coconut shell [5]. Many efforts [6,7] have been expended during the last decade to produce activated carbons from agricultural by-products such as fruit stones and straw wastes in order to obtain a cheaper, more cost effective product. Indeed, Patrick and Streat [8] prepared activated carbons from wheat straw wastes although the details of the preparation conditions were not specified, and showed that the obtained activated carbon exhibited adsorption properties comparable to those of commercial ones.

In general, the manufacturing processes of activated carbons in laboratory scale may be categorized into two groups. That is, one includes the synchronous process of carbonization and activation (denoted the one-stage process), the other is the asynchronous process in which a separate carbonization process is included prior to the activation process (denoted the two-stage process) [9]. If the precursor is heat treated by one of the above-mentioned two processes, the resultant activated carbons should naturally have different burn-off ratios and thus different pore characteristics and adsorption capacities since the two processes have definite differences in thermal history. Considering that the burn-off itself is a dependent function on the heat treatment history, either the burn-off or the heat treatment conditions may not be an appropriate single parameter to consider the effect of thermal history on the various characteristics of activated carbons. This implies that a more objective parameter should be considered in order to take into account the effect of thermal history on the porosity development in activated carbons.

It has been widely accepted that the pore structure and adsorption properties of activated carbons are strongly influenced by physico-chemical nature of precursor materials and the heat treatment profile, i.e. thermal history during the manufacturing process. Numerous works have thus been devoted to studying the influence of the precursor and the preparation conditions inclusive of carbonization and activation on the pore characteristics and

*Corresponding author. Tel.: +82-2-880-8030; fax: +82-2-885-1748.

E-mail address: crpark@gong.snu.ac.kr (C.R. Park).

0008-6223/01/$ – see front matter
PII: S0008-6223(00)00163-9

adsorption properties of resultant activated carbons on the pore characteristics and adsorption properties of resultant activated carbons [10]. However, little has been studied systematically the effect of thermal history on the porosity evolution in terms of structural parameters of precursor carbons.

It is thus the main purpose of this study to elucidate the effect of pre-carbonization on the porosity development in activated carbons. To consider the thermal history effect more objectively, we used normalized parameters obtained by dividing the general porosity parameters by the total burn-off ratio. It was an additional aim of this work to establish the preparation conditions of activated carbons from rice straws which can be a good feedstock for cheaper activated carbons.

2. Experimental

2.1. Precursor material

Rice straws as the precursor materials were chopped to about 3 cm in length and used after oven-drying at 110°C for 3 h. The proximate analyses of the rice straws are shown in Table 1.

2.2. Preparation of activated carbons

Activated carbons were produced by two different processes of which thermal history was shown in Fig. 1; in the one-stage process (Fig. 1(a)) the precursor was heated under N_2 at a rate of 10°C/min to a specified temperature in the range of 700–900°C and kept at the same temperature under CO_2 for a specified time to yield activated carbons (denoted S1AC). On the other hand, in the two-stage process (Fig. 1(b)) the precursor was first carbonized under N_2 at 900°C for 1 h, and cooled down to room temperature. The activation of the carbonized char sample was carried out according to exactly the same heat treatment profile with that of the one-stage process; the resultant activated carbons were denoted as S2AC. That is, the only difference between the two processes is the inclusion of a separate carbonization process prior to the activation in order to examine the effect of pre-carbonization on the porosity development. Throughout the heat treatment process, the flow rate of N_2 and CO_2 was fixed at 1 *l*/min. After heat treatment, the furnace was cooled under N_2 to room temperature to prevent further oxidation of the sample. All the samples obtained were powdered to sizes less than 65 μm.

Table 1
Proximate analyses of rice straws

Elemental analysis (%)		Component analysis (%)	
C	39.8	Extractives	9.8
H	5.5	Holocellulose	61.6
O	53.8	α-cellulose	34.1
N	0.9	Lignin	14.8
		Ash	15.0

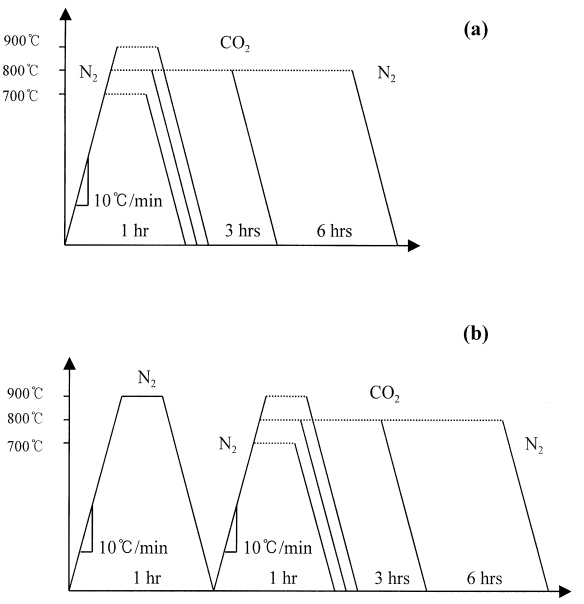

Fig. 1. Thermal history in (a) the one-stage and (b) the two-stage processes.

2.3. Characterizations

The total burn-off ratio was obtained from the ratio of the weight loss during the whole heat-treatment processes to the dry weight of the precursor. Nitrogen adsorption isotherms at 77 K were obtained using Micromeritics instrument (Model ASAP 2010) in the relative pressure ranging from 10^{-6} to 1. Before the measurement all the samples were degassed at 150°C for 1 h. The adsorption data were analyzed by the BET equation and the procedure developed by Barrett et al. [11] to calculate the BET surface area, the mean pore diameter, and the pore size distribution, respectively. The single point total pore volume was determined from the amount of nitrogen adsorbed at the relative pressure of 0.95. The pore volumes of micro, meso, and macropores were calculated from the following equations:

Micropore volume = Single point total pore volume
− (Cumulative BJH total pore volume − Cumulative BJH pore volume larger than the pore diameter at the relative pressure of 0.95) (1)

Mesopore volume = Cumulative BJH pore volume larger than the pore diameter of 2 nm − Cumulative BJH pore volume larger than the pore diameter of 50 nm (2)

Macropore volume = Single point total pore volume − micropore volume − mesopore volume (3)

In this work, 2 and 50 nm were taken as the boundary sizes between micro and mesopore, and meso and macropore, respectively [12]. The pore size distribution curve was obtained from the BJH analysis of the experimental nitrogen adsorption/desorption isotherm [11], which gives the plot $dV/d\log(D)$ vs. D, where V is the cumulative pore volume and D is the pore diameter.

The mean pore diameter was calculated using the following equation:

$$\text{Mean pore diameter (Å)} = \frac{4V}{A}$$

where, V is the single point total pore volume at the relative pressure of 0.95 and A is the BET surface area.

The structural changes in the sample during the heat treatment process were monitored using the Ni-filtered CuKI radiation on the MXP 18X-MF22-SRA X-ray diffractometer operating at 100 mA and 50 kV. After the peak-deconvolution of the obtained X-ray diffractograms, various structural parameters were determined with a conventional method [13]. The ash content of samples was determined according to ASTM D 2866-83. In essential, exact 0.3 g of the sample was placed to a crucible and heated at 650°C for 12 h in the stream of air. The ash content was calculated using the following equation:

$$\text{Ash (\%)} = \frac{(D-B)}{(C-B)} \times 100 \quad (4)$$

where, B is the weight of crucible, C is the weight of crucible plus original sample, and D is the weight of crucible plus ashed sample.

3. Results and discussions

3.1. Adsorption/desorption isotherms and porosity development

Fig. 2 represents the nitrogen adsorption/desorption isotherms at 77 K of both S1AC and S2AC as a function of activation temperature. Except for the higher adsorption capacity of S2AC, the overall shapes of the adsorption isotherms are quite similar to each other. The isotherms of the activated carbons prepared at 700°C are of Type I, indicative of the microporous character. However, as the activation temperature increases, the knee of isotherm becomes more rounded, and the hysteresis effect and the slope of the plateaus increase to yield Type IV isotherms, indicating the presence of mesopores. Indeed, the carbons activated at 800°C exhibit the most prominent hysteresis effect which may be characterized by the formation of slit-shaped pores [14]. The activated carbons obtained at 900°C show the decreased nitrogen uptake and the isotherm of more rounded shape at high relative pressure range. The BET surface areas and pore diameters of the two types of activated carbons, calculated from the adsorption isotherms of Fig. 2, are listed in Table 2. The maximum values of BET surface areas for both S1AC and

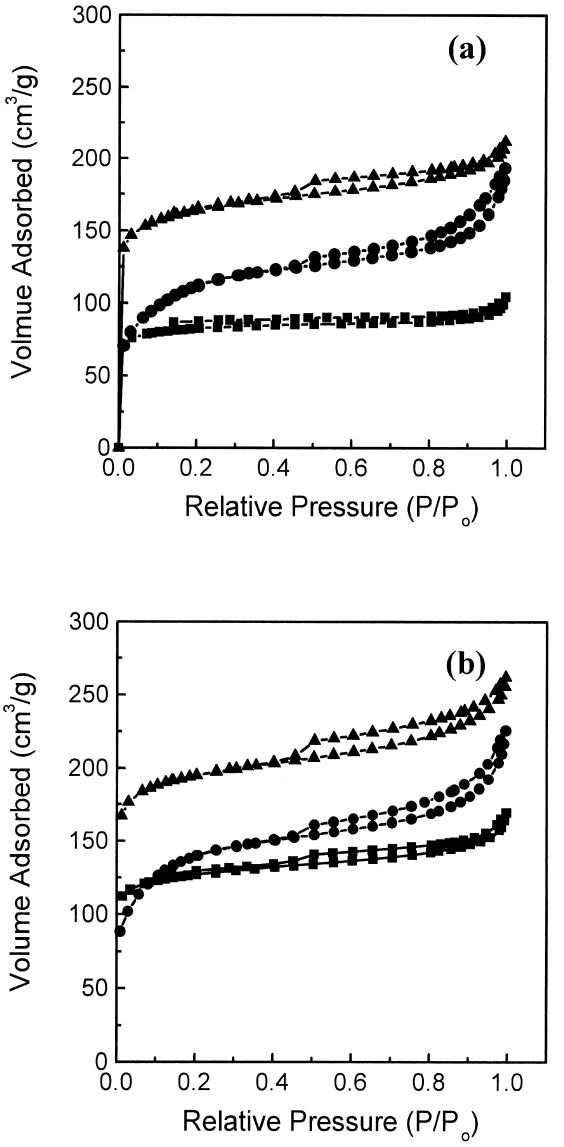

Fig. 2. Adsorption/desorption isotherms of nitrogen at 77 K onto (a) S1AC and (b) S2AC as a function of activation temperature. (Activation time = 1 h; ■: 700°C, ▲: 800°C, ●: 900°C).

Table 2
BET surface areas and pore diameter of activated carbons

Sample code		S1AC		S2AC	
Temp. (°C)	Time (h)	Surface area (m^2/g)	Pore diameter (Å)	Surface area (m^2/g)	Pore diameter (Å)
700	1	280	21.3	490	22.9
800	1	550	22.5	650	23.4
800	3	680	23.9	790	24.1
800	6	530	26.2	780	25.4
900	1	400	26.9	480	25.7

S2AC are obtained at the activation temperature of 800°C, however the pore diameter increases as the activation temperature increases. This may possibly be an indication that up to 800°C, somewhat disorganized carbons or residual tar materials are eliminated by the opening of closed pores, however, above 800°C the existing pores are widened or coalesced to larger pores by gasification of carbons in the pore walls [15]. Comparing the two different processes, until 800°C, the pore diameter of S2AC is slightly larger than that of S1AC, however above 800°C the situation is reversed. This result suggests that in S2AC the pore widening occurring up to 800°C may arise from the opening or widening of the pores created during pre-carbonization process. However, due to comparatively stable carbon structures formed during pre-carbonization, the pore-widening is somewhat suppressed at the subsequent further heat treatment. Meanwhile, in S1AC, relatively larger pores are formed during activation at higher temperatures due to comparatively labile carbons.

The above observation suggests that, when the activation time is fixed at 1 h, the initially formed micropores develop to mesopores or macropores as the heat treatment temperature increases. Considering that S2AC exhibits the higher adsorption capacity, it may be deduced that the pore widening is somewhat deterred in the two-stage activated carbons. Indeed, as can be seen clearly from Fig. 3, the micropores smaller than about 20 Å in diameter increases rapidly up to 800°C for both S1AC and S2AC, the extent of which is much greater in S2AC. Above 800°C, the micropores in S1AC develop to mesopores of the diameter ranging from 100 to 600 Å (Fig. 3a), while in the case of S2AC the development of mesopores is not appreciable, despite of the decrease in the micropores. This result suggests obviously that the micropores in S1AC take part more easily in the pore widening process than in S2AC.

Fig. 4 represents the effect of activation temperature on the pore volume distribution in the two types of activated carbons. It can be clearly seen that the micropore volume reaches maximum value at 800°C, whereas the mesopore volume increases linearly with the activation temperature. This tendency does not change even after the normalization procedure although the absolute values increase slightly since the total burn-off ratio is less than unity. The above observation suggests that the pore-drilling and pore-widening by an activating agent occur simultaneously up to 800°C to increase the micro and mesopore volumes, however, the pore-widening effect exceeds the pore drilling effect by the gasification above 800°C that destroys the pore walls of micropores.

A similar tendency to the above observation was also found as shown in Fig. 5. That is, the nitrogen uptakes of both S1AC and S2AC increase as the activation time increases at the fixed heat treatment temperature of 800°C. It should however be noted that S1AC exhibits a maximum uptake of nitrogen at the activation time of 3 h whereas S2AC shows somewhat saturated nitrogen-uptake of much higher values than that of S1AC. This indicates that the prolonged activation promotes both pore-drilling and pore-widening to develop meso and macroporosity in the two types of activated carbons. Indeed, in Fig. 6, which represents the pore size distribution of the two types of activated carbons as a function of the activation time, it can be clearly seen that, as the activation time increases, there is an appreciable development of the mesopores of the diameter ranging from 100 to 1000 Å in S1AC (Fig. 6(a)) while there is comparatively less appreciable development of mesopores that has much smaller diameter ranging from 60 to 600 Å in S2AC (Fig. 6(b)). In addition, as shown in Fig. 7, there is a remarkable contrast in the micropore volume between S1AC and S2AC. In the case of S1AC (Fig. 7(a)), the micropore volume decreases considerably with the increase of activation time, while the mesopore volume increases gradually. In contrast, for S2AC (Fig. 7(b)), the micropore volume rarely decreases even when the activation time increases. This result suggests again that the carbons in S1AC are relatively labile to gasification reaction probably due to less well-organized carbon structure [16], and hence the micropores developed in the early stage of heat treatment are somewhat easily widened and collapsed to larger pores. In contrast, the carbons in S2AC are relatively stable, which may ensure gentle gasification by preventing an abrupt collapse of carbon structures.

The above observation indicates that, although both pore-drilling and pore-widening are driving forces operating simultaneously in creating pores during activation,

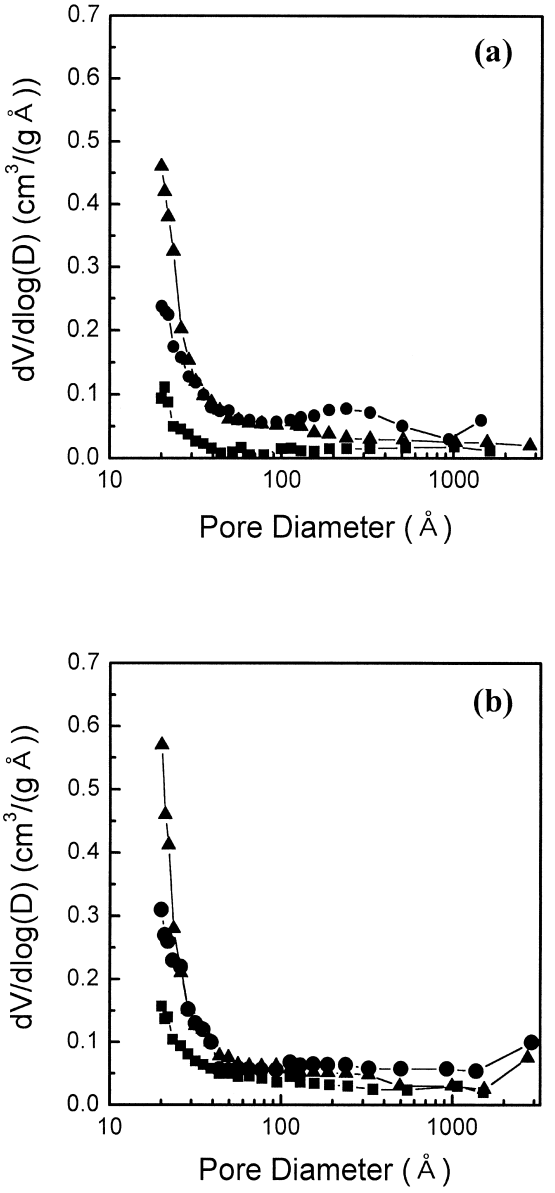

Fig. 3. Pore size distribution of (a) S1AC and (b) S2AC as a function of activation temperature. (Activation time = 1 h; ■: 700°C, ▲: 800°C, ●: 900°C).

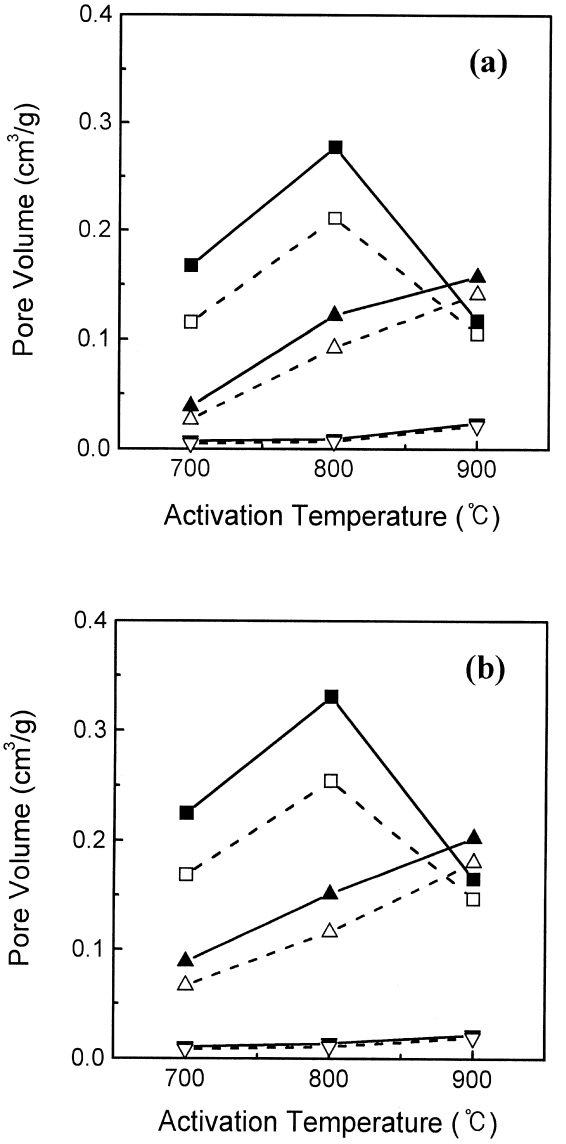

Fig. 4. Effect of pre-carbonization on the pore volumes of (a) S1AC and (b) S2AC as a function of activation temperature. (Activation time = 1 h); unnormalized (dashed line) and normalized (solid line) volumes of micropore (■, □), mesopore (▲, △), and macropore (▼, ▽).

pore-drilling is comparatively more dominant in S2AC than in S1AC. With this observation it may be possible to conclude that the introduction of pre-carbonization process produces relatively stable carbons that may promote preferentially pore-drilling to pore-widening as in the case of S2AC.

3.2. Structural change with porosity development

It has been generally known that the rate of the gasification of carbons with oxidizing gases is considerably influenced by various factors such as concentration of active site, structure of carbon, inorganic impurities, and diffusion rate of gases [17]. Pastor et al. [18] indicated that the structure of carbon is the most important among these factors: the carbon of well-organized and dense aromatic structure has less reactive sites and less abrupt decomposition. The reactivity of graphitizing and non-graphitizing carbons to oxidizing gases, such as carbon dioxide and oxygen, decreases with increasing heat treatment tempera-

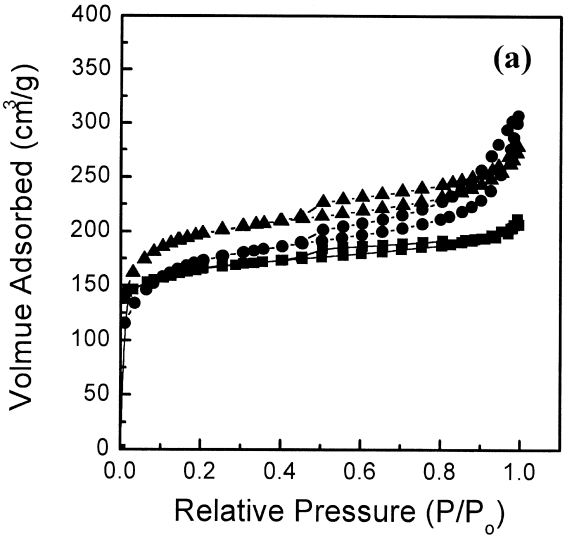

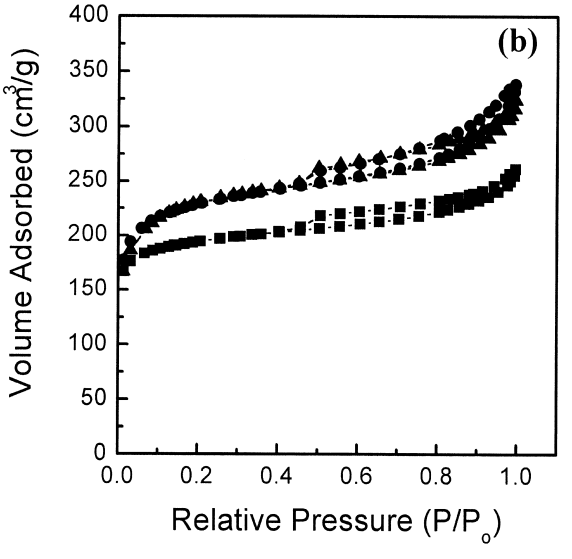

Fig. 5. Adsorption/desorption isotherms of nitrogen at 77 K onto (a) S1AC and (b) S2AC as a function of activation time. (Activation temp.=800°C; ■: 1 h, ▲: 3 h, ●: 6 h).

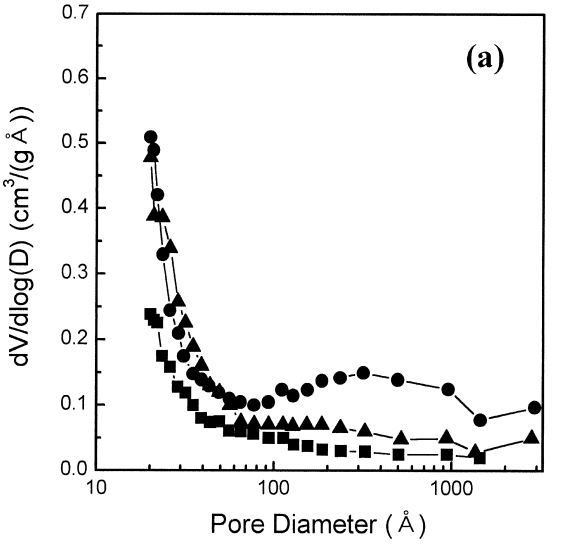

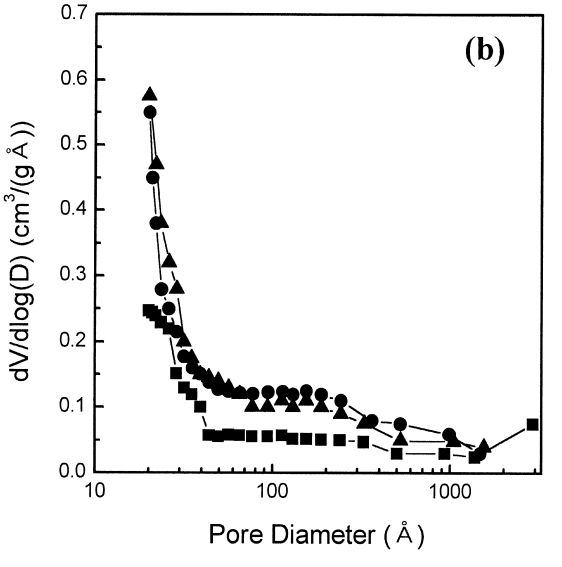

Fig. 6. Pore size distribution of (a) S1AC and (b) S2AC as a function of activation temperature. (Activation temp.=800°C; ■: 1 h, ▲: 3 h, ●: 6 h).

ture because thermal annealing due to heat treatment results in the reduction of structural defects [19].

It was indeed suggested from the results observed hitherto that the better pore characteristics of S2AC might arise from the more stable carbon structure than S1AC. To confirm this point, X-ray diffractometry was carried out for the samples heat treated at 900°C for 1 h, the results of which were shown in Fig. 8. It can be clearly seen that, after pre-carbonization of rice straws, the peaks at 2T.16 and 22E, characteristic of cellulose crystallites in rice straws disappear and the two broad peaks show up newly near 2T.26 and 44E. These new two peaks that arise from the carbon layer structures can be attributed to (002) and (10) reflections of the graphitic structure [20]. The sharp peaks at 2T.21 and 40E are considered due to the crystallites of some inorganic impurities, for example silicon oxide, in rice straws [21]. The nature of impurities and their role in porosity evolution will be reported in the near future.

It should be noted obviously from Fig. 8 that the one-stage process produces activated carbons of a negligible amount of carbon structures (Fig. 8(c)), however,

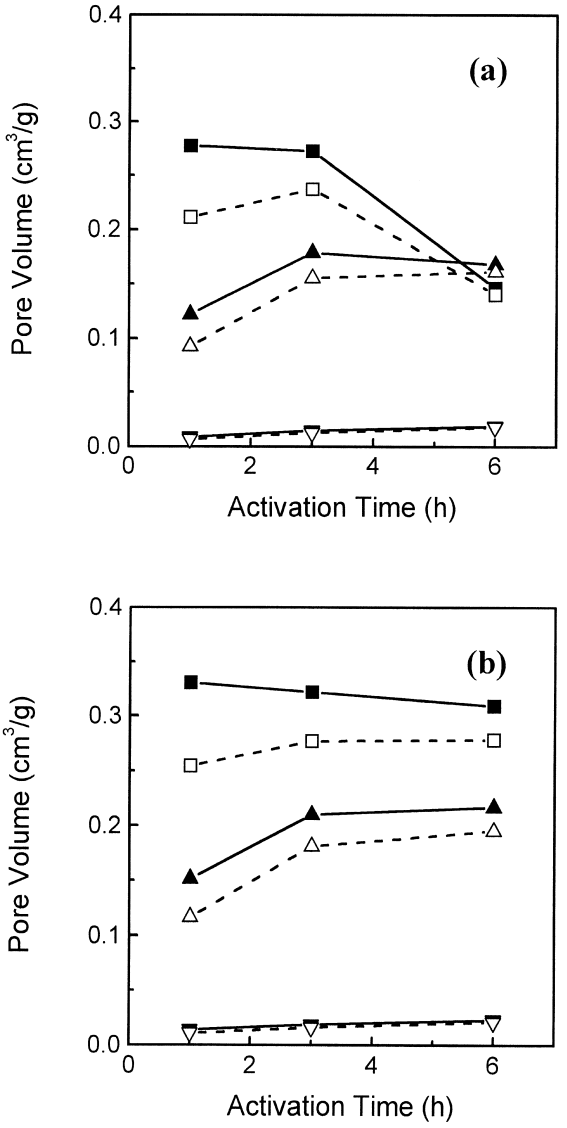

Fig. 7. Effect of pre-carbonization on the pore volumes of (a) S1AC and (b) S2AC as a function of activation time. (Activation temp.=800°C); unnormalized (dashed line) and normalized (solid line) volumes of micropore (■, □), mesopore (▲, △), and macropore (▼, ▽).

considerable amount of carbon structures formed by the pre-carbonization (Fig. 8(b)) still survives in the case of two-stage process (Fig. 8(d)). This indicates strongly that the pre-carbonization produces the char consisting of relatively well-organized aromatic carbons with sp^2 bonding character, which are more stable than somehow amorphous-like carbons of sp^3 bonding character to gasification reaction by oxidizing agent such as carbon dioxide. Table 3 indeed shows that much less amount of carbons are left after activation for 6 h at 800°C in S1AC than in S2AC, indicative of the more stable carbon structures of

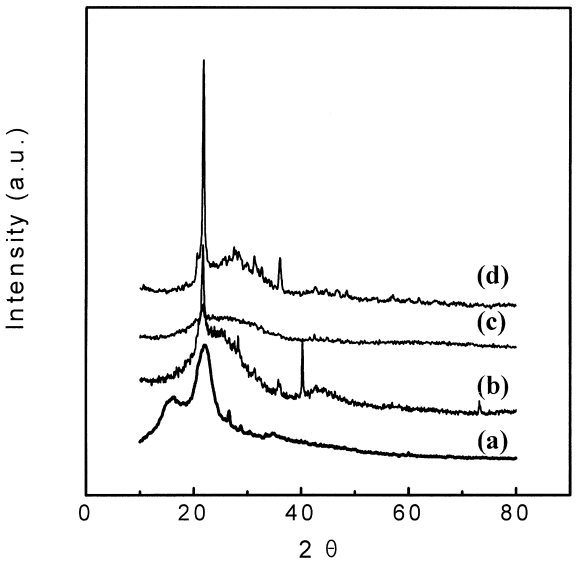

Fig. 8. X-ray diffractograms of (a) rice straws, (b) pre-carbonized, (c) S1AC, and (d) S2AC heat treated at 900°C for 1 h.

S2AC. It may be natural to conclude at this juncture that such relatively stable carbons are more resistant to an abrupt decomposition during activation, and hence lead to the formation of micropores of high adsorption capacity.

Table 4 summarizes the structural parameters of both S1AC and S2AC, calculated from the peak analysis of diffractograms shown in Fig. 8. The interesting feature is that the values of L_c and d_{002} are quite similar, despite of the differences in thermal histories of S1AC and S2AC, however, the $L_{a\perp}$ value of S2AC is much large as twice as that of S1AC. Moreover, the $L_{a\perp}$ value becomes negligibly small with the prolonged heat treatment. This result strongly suggests two distinctive points: one is that pores are created by the decomposition of carbon structure along the *a*-direction and the other that the pre-carbonization ensures the formation of much stable carbon structures in S2AC.

4. Conclusions

With the inclusion of pre-carbonization process prior to the activation process, cheaper and high performance activated carbons could be prepared from rice straws. It was found that the inclusion of pre-carbonization process contributes to the formation of activated carbons with higher values of the BET surface area and microposity than those of activated carbons without pre-carbonization. From this observation, it can be concluded that the inclusion of pre-carbonization process is necessary to get a relatively less defective carbonaceous intermediate that yields high content of micropores during the subsequent

Table 3
Ash content and elemental composition

Sample code		S1AC					S2AC				
Temp. (°C)	Time (h)	Ash (%)	C	H	N	$O^{diff.}$	Ash (%)	C	H	N	$O^{diff.}$
				(%)					(%)		
800	1	34.2	53.8	0.5	0.6	45.1	30.4	56.1	0.6	0.7	42.6
800	6	73.3	25.1	0.2	0.8	73.9	48.0	44.8	0.3	0.7	54.2
							(30.5)[a]	(57.6)	(0.7)	(0.8)	(40.9)

[a] The value in bracket is for the pre-carbonized sample.

Table 4
Structural parameters of activated carbons

Sample code		S1AC			S2AC		
Temp. (°C)	Time (h)	d_{002} (Å)	L_c (Å)	$L_{a\perp}$ (Å)	d_{002} (Å)	L_c (Å)	$L_{a\perp}$ (Å)
800	1	3.65	9.03	15.54	3.53	9.69	29.25
800	3	3.41	9.52	11.21	3.43	9.81	19.34
800	6	3.40	10.86	n.s.[b]	3.40	10.86	n.s.
900	1	3.48	8.39	n.s.	3..41	10.21	n.s.
					(3.53)	(9.79)	(23.25)[a]

[a] The value in bracket is for the pre-carbonized sample.
[b] Undetermined due to negligibly small intensity of (10) reflection.

activation of rice straws. Also was found that 800°C, 3 h were the optimum activation time within the experimental range for the preparation of high performance activated carbons from rice straws. This could be attributed to the fact that, although pore-drilling and pore-widening occur simultaneously to increase the micro and mesopore volumes to the activation temperature of 800°C, pore-widening effect was however dominant above 800°C, leading to the increase of mesopore volume.

Acknowledgements

The authors are thankful for the financial support by Korea Institute of Industrial Technology Evaluation and Planning (ITEP), Ministry of Commerce Industrial and Energy (Profile no. B18-961-5401-16-2-3).

References

[1] Jagtoyen M, Derbyshire F. Activated carbons from yellow poplar and white oak by H_3PO_4 activation. Carbon 1998;36(7–8):1085–97.
[2] Verheyen V, Rathbone R, Jagtoyen M, Derbyshire F. Activated extrudates by oxidation and KOH activation of bituminous coal. Carbon 1995;33(6):763–72.
[3] Pandolfo AG, Amini-Amoli M, Killingley JS. Activated carbons prepared from shells of different coconut varieties. Carbon 1994;32(5):1015–28.
[4] John JF, John BT, Sing JSW. Adsorption of nitrogen and water vapour by activated Nomex chars. Carbon 1995;33(6):795–9.
[5] Raveendran K, Ganeshn A. Adsorption characteristics and pore-development of biomass-pyrolysis char. Fuel 1998;77(7):769–81.
[6] Sai PMS, Ahmed J, Krishnaiah K. Rebuttal to comments on production of activated carbon from coconut shell char in a fluidized bed reactor. Ind Eng Chem Res 1999;38(3):1169–71.
[7] Rodriguez-Reinoso F, Molina-Sabio M, Gonzalez MT. The use of steam and CO_2 as activating agents in the preparation of activated carbons. Carbon 1995;33(1):15–23.
[8] Patrick JW, Streat M. In: Extended Abstracts, 22nd biennial conf. on carbon, UC San Diego (California. USA): American Carbon Society, 1995, pp. 404–5.
[9] Molina-Sabio M, Gonzalez T, Rodriguez-Reinoso F, Sepulvelda-Escribano A. Effect of steam and carbon dioxide activation in the micropore size distribution of activated carbon. Carbon 1996;34(4):505–9.
[10] Gregova K, Eser S. Effects of activation method on the pore structure of activated carbons from apricot stones. Carbon 1996;34(7):879–88.
[11] Barrett EP, Jaoyner LG, Halenda PP. The determination of pore volume and area distributions in porous substances. I. Computations from nitrogen isotherms. J Am Chem Soc 1951;73:373–80.
[12] IUPAC. Manual of symbols and terminology, Appendix 2, Pt. 1: Colloid and surface chemistry. Pure Appl Chem 1972;31:578.
[13] Dobb MG, Johnson DJ, Park CR, Guo H. Structure-compressional property relations in carbon fibres. Carbon 1995;33(11):1553–9.

[14] Gregg SJ, Sing KSW, Adsorption, surface area and porosity, London: Academic Press, 1982, p. 287.
[15] Wigman T. Industrial aspects of production and use of activated carbons. Carbon 1989;27(1):13–22.
[16] Gribanov AV, Sazanov YN. Carbonization of polymers. Russ J Applied Chem 1996;70(6):839–60.
[17] Rodriguez-Reinoso F. Controlled gasification of carbon and pore structure development. In: Lahaye J, Ehburger P, editors, Fundamental issues in control of carbon gasification reactivity, Netherlands: Kluwer Academic, 1991, pp. 533–65.
[18] Pastor AC, Rodriguez-Reinoso F, Marsh H, Martinez MA. Preparation of activated carbon cloths from viscous rayon. Part I. Carbonization procedures. Carbon 1999;37(8):1275–83.
[19] Marsh H, Kuo K. Kinetics and catalysis of carbon gasification. In: Marsh H, editor, Introduction to carbon science, London: Butterworths, 1989, pp. 107–51.
[20] Babu VS, Seehra MS. Modeling of disorder and X-ray diffraction in coal-based graphitic carbons. Carbon 1996;34(10):1259–65.
[21] Kumar B, Godkhindi MM. Studies on the formation of SiC, $Si_3N_4$and Si_2N_2O during pyrolysis of rice husk. J Mat Sci Lett 1996;15(5):403–5.